Available online at www.sciencedirect.com
SCIENCE DIRECT®
Journal of Computational Physics 190 (2003) 249–274
JOURNAL OF COMPUTATIONAL PHYSICS
www.elsevier.com/locate/jcp

Coupling of atomistic and continuum simulations using a bridging scale decomposition

Gregory J. Wagner *,[1], Wing Kam Liu

Department of Mechanical Engineering, Northwestern University, 2145 Sheridan Rd., Evanston, IL 60208, USA

Received 20 August 2002; received in revised form 20 March 2003; accepted 20 May 2003

Abstract

We present a new method for coupling molecular dynamics (MD) and continuum mechanics simulations that is based on the projection of the MD solution onto the coarse scale shape functions. This projection, or "bridging scale", represents that part of the solution that is obtainable by both solution methods. By subtracting the bridging scale from the total solution, we arrive at a coarse-fine decomposition that, by a proper choice of projection operator, decouples the kinetic energy of the two simulations. The resulting decomposition can be used in a finite-temperature simulation method in which MD is used only in a localized region, while the continuum simulation covers the entire domain, including the MD region to which it is coupled. One major advantage of this approach is that separate time step sizes can be used in the two simulations, so that the coarse scale time step is not limited to the time scale of the atomic vibrations present in the fine scale. Example problems are demonstrated on a 1D lattice, for which the method is shown to be accurate both for harmonic and anharmonic interatomic potentials.

Keywords: Multiple-scale simulations; Molecular dynamics; Finite elements; Bridging scale; Coupling methods

1. Introduction

Thanks to the ever-increasing power and affordability of fast computers and the development of accurate interatomic potentials for a range of materials, classical molecular dynamics (MD) simulations have become prominent as a tool for elucidating complex physical phenomena. With the ability to examine atomic-scale dynamics in great detail, researchers have used MD to gain new insight into problems that have been resistant to theoretical solution, such as solid fracture [1], surface friction [2], and plasticity [3]. However, the length and time scales that can be probed using MD are still fairly limited. For example, a 10 nm cubic domain of a metal can be simulated only for times less than around 10^{-10} s, even on very large parallel machines [3].

* Corresponding author.
E-mail addresses: g-wagner@northwestern.edu (G.J. Wagner), w-liu@northwestern.edu (W.K. Liu).
[1] Present address: Sandia National Laboratories, Livermore, CA 94551-9950, USA.

0021-9991/$ - see front matter
doi:10.1016/S0021-9991(03)00273-0

Nomenclature

$\tilde{\mathbf{a}}_2$	difference between accelerations of region 2 atoms due to a force f^*, and the actual coarse scale accelerations
$\mathbf{d}$	vector of displacement degrees of freedom at coarse scale nodes
$\mathbf{f}$	vector of interatomic forces
$\mathbf{f}^*$	interatomic force evaluated with $\mathbf{u}'_2$ set to zero
$\hat{\mathbf{f}}$	total force on atoms including effects of removed fine scale degrees of freedom
$\bar{\mathbf{F}}$	coarse scale deformation gradient
$\mathbf{K}_2$	stiffness matrix relating fine scale displacements in region 2 to atomic forces
$\mathbf{K}_{12}, \mathbf{K}_{22}$	stiffness matrices relating fine scale displacements in region 2 to atomic forces in regions 1 and 2, respectively
L	total Lagrangian of system
m	number of fine scale subcycles for time integration
m_α	mass of atom α
$\mathbf{M}_A$	diagonal mass matrix containing atomic masses
$\mathbf{M}$	coarse scale mass matrix
$\mathscr{M}$	fine scale mass matrix
n_a	total number of atoms in the domain
n_c	number of coarse scale nodes in the domain
$\mathbf{N}$	matrix of coarse scale shape functions: $N_{I\alpha}$ gives shape function of node I evaluated at atom α
$\mathbf{P}$	coarse scale projection matrix
$\mathbf{P}^K$	first Piola–Kirkhoff stress
$\mathbf{q}$	vector of displacements at atoms computed in an MD simulation
$\mathbf{Q}$	fine scale projection operator
$\mathbf{R}, \mathbf{R}_\beta$	random forces capturing temperature effects at MD boundary
s	Laplace transform variable
t	time
$\Delta t, \Delta t_m$	coarse and fine scale time steps for time integration ($\Delta t_m = \Delta t/m$)
$\mathbf{u}$	vector of displacement degrees of freedom at atoms
$\bar{\mathbf{u}}, \mathbf{u}'$	vectors of coarse and fine scale parts of total displacements at atoms, respectively
$U(\mathbf{u})$	potential energy function
ΔV_α	volume of domain surrounding atom α
$\mathbf{X}_\alpha$	initial or material coordinates of atom α
$\boldsymbol{\beta}$	time integral of θ
$\tilde{\boldsymbol{\beta}}$	damping kernel matrix in the generalized Langevin equation (GLE)
$\boldsymbol{\theta}$	time history kernel matrix capturing effects of region 2 fine scales

Increases in this simulation time require a proportional reduction in the number of atoms simulated. The results of such a simulation therefore can rarely be compared directly to experiments, since laboratory observations of these sorts of mechanical phenomena are usually made on much larger length and time scales. Furthermore, the relevance of simulations on such small time scales can be called into question. For example, in studies of plasticity or fracture, MD can simulate strain rates only as low as around 10^6 s^{-1} [3], an artificially high value; meanwhile, it is known that real systems show strain rate-dependent behavior even at much lower strain rates. New methods that can extend length and time limits of MD are needed.

One possible approach that can be applied to many problems is to use MD only in localized regions in which the atomic-scale dynamics are important, and a continuum simulation method (such as finite

elements) everywhere else. This general approach has been taken by several different groups of researchers. Abraham et al. [4,5] have developed a coupled finite elements, MD, tight-binding (FE/MD/TB) method in which the three methods are used concurrently in different regions of the computational domain. In this method, the finite element mesh is graded down to the atomic lattice size in an overlap, or "handshake", region; the dynamics is governed by a total Hamiltonian function that combines the separate Hamiltonians of the three regions in an appropriate way. This approach has been effective in the simulation of brittle fracture. Another method developed recently is the quasicontinuum method [6–11], in which atomic degrees of freedom are selectively removed from the problem by interpolating from a subset of representative atoms, similar to finite element interpolation. Adaptivity criteria are used to reselect these representative lattice points in regions of high deformation, so that where necessary (e.g., near a dislocation) full atomic resolution is recovered. This approach has found application to simulations of dislocation motion [6,7], grain boundary interaction [8], nanoindentation [7], and fracture [9,10]. The method has been used mainly for quasistatic deformation at zero temperature, although Shenoy et al. have suggested an extension to finite temperature problems using a Monte Carlo technique [12].

A problem with multiple-scale simulations that has not been addressed satisfactorily is that of multiple time scales. In general, methods that couple finite elements to MD for dynamic, finite temperature simulations are limited in their time step size to that used for the MD part of the domain, even though the large scale variables change much more slowly. This is largely due to the fact that the finite element mesh is graded down to the atomic lattice scale at the boundary between the continuum and MD domains, so that finite element nodes coincide with atoms. The time step for the continuum simulation is limited to the time step that is stable for the smallest elements in the mesh.

In this work, we present a new method that allows the coupling of finite elements (or other continuous interpolation functions, such as meshfree shape functions [13]) to MD simulations without the need to grade the continuum nodal spacing down to the atomic lattice size. This method is based on a decomposition of the displacement field $\mathbf{u}$ into coarse and fine scales:

$$\mathbf{u} = \bar{\mathbf{u}} + \mathbf{u}', \tag{1}$$

where $\bar{\mathbf{u}}$ is a coarse scale that can be represented by a set of basis functions (such as finite element shape functions), and $\mathbf{u}'$ is a fine scale whose projection onto the coarse scale basis is zero. This sort of scale decomposition is common in the analysis of turbulent fluid flow; for example, it has been used by Hughes and coworkers [14,15] for solid mechanics in the variational multiscale method.

In our approach, the coarse scale is represented *everywhere* in the domain, including regions where MD will also be used, by a continuous interpolation. In the regions of the domain designated for MD simulation, the fine scale $\mathbf{u}'$ can be gleaned from the MD solution by first subtracting off the projection of the MD solution onto the coarse scale basis. This projection, or "bridging" scale, removes from the simulation the information contained in both the continuum and MD parts of the solution. Coarse scale momentum and energy are easily transfered out of the MD regions, since the coarse scale representation co-exists with the fine scale in those regions. This bridging scale approach was originally used by Liu et al. [16] to enrich the finite element method with meshfree shape functions. It was later used by Wagner and Liu [17,18] for applying essential boundary conditions in meshfree computations.

Section 2 of this paper concerns the formal decomposition of the total solution into coarse and fine scales. We present the formulation of the coarse-fine decomposition using the bridging scale projection, without yet taking into account the fact that our eventual goal is to compute the fine scale only in a localized region of the domain. We address the details of implementing the coarse-fine decomposition in the remaining sections of the paper. In Section 3, we discuss the repercussions of limiting the fine scale computation to a small region of the domain. Through the formal elimination of the uncomputed fine scale degrees of freedom, we derive a generalized Langevin equation [19,20] for the atoms at the boundary of the computed region in terms of both scales of the computation, providing a coupling

between the two simulations. We also outline a method for computing the stress in the coarse scale region based on the interatomic potential at the fine scale, and show that the resulting equation for the coarse scale is equivalent to the standard weak form of the momentum equation used in finite elements. A detailed time integration algorithm is presented in Section 4 that allows a smaller time step size (and proportionately more frequent steps) to be used in the fine scale region than in the coarse scale. This approach takes advantage of the slower time scale of the coarse simulation. In Section 5, the method is applied to the simulation of wave propagation in a 1D lattice, in which only a part of the lattice is represented by molecular dynamics. It is shown that the solution is indistinguishable from the full MD solution for the case of a harmonic lattice, and gives reasonable accuracy even when the forces between atoms are nonlinear. We conclude in Section 6 with an assessment of the method and directions for future research.

2. Formulation

2.1. Coarse-fine decomposition

Consider a set of n_a atoms representing a body. Let the displacement of an atom α be denoted by $\mathbf{u}_\alpha$. The displacement is to be decomposed into a coarse scale $\bar{\mathbf{u}}_\alpha = \bar{\mathbf{u}}(\mathbf{X}_\alpha)$, where $\mathbf{X}_\alpha$ is the initial position of atom α, and a fine scale $\mathbf{u}'_\alpha$. Note that while the coarse scale can be thought of as a continuous displacement field and can technically be interpolated at points in between atoms, the fine scale and therefore the total displacement are discrete functions that are defined only at atomic positions. In this paper, we will consistently use Greek indices $(\alpha, \beta, \gamma, \ldots)$ to distinguish atoms, and uppercase Roman indices $(I, J, K, \ldots)$ to label coarse scale nodes.

The coarse scale is to be represented by a set of basis functions, such as finite element or meshfree shape functions, defined on a set of n_c nodes. We therefore write the coarse scale, interpolated at the position of an atom, as

$$\bar{\mathbf{u}}(\mathbf{X}_\alpha) = \sum_I N_I^\alpha \mathbf{d}_I, \tag{2}$$

where $N_I^\alpha = N_I(\mathbf{X}_\alpha)$ is the shape function associated with node I evaluated at $\mathbf{X}_\alpha$, and $\mathbf{d}_I$ is the displacement degree of freedom at node I. The summation in (2) is over all of the n_c coarse scale nodes in the domain, as are all such summations in this section.

It will be convenient to use a matrix representation for (2) and subsequent equations. Quantities such as $\mathbf{u}_\alpha$, $\bar{\mathbf{u}}_\alpha$, and $\mathbf{d}_I$ can be represented as column vectors containing all of the spatial components at each quantity at each atom or node. For instance, in three dimensions

$$\mathbf{u} = \begin{Bmatrix} u_{1x} \\ u_{1y} \\ u_{1z} \\ u_{2x} \\ \vdots \\ \vdots \\ u_{n_a z} \end{Bmatrix}, \qquad \mathbf{d} = \begin{Bmatrix} d_{1x} \\ d_{1y} \\ d_{1z} \\ d_{2x} \\ \vdots \\ d_{n_c z} \end{Bmatrix}, \tag{3}$$

where, e.g., u_{1x} is the x component of $\mathbf{u}(\mathbf{X}_1)$. Eq. (2) can then be written in matrix form

$$\bar{\mathbf{u}} = \mathbf{N}\mathbf{d} \tag{4}$$

if the shape function matrix $\mathbf{N}$ is taken to be

$$\mathbf{N} = \begin{bmatrix} N_1^1\mathbf{I}_{3\times3} & N_2^1\mathbf{I}_{3\times3} & \dots & N_{n_c}^1\mathbf{I}_{3\times3} \\ N_1^2\mathbf{I}_{3\times3} & N_2^2\mathbf{I}_{3\times3} & \dots & N_{n_c}^2\mathbf{I}_{3\times3} \\ \vdots & \vdots & \ddots & \vdots \\ N_1^{n_a}\mathbf{I}_{3\times3} & N_2^{n_a}\mathbf{I}_{3\times3} & \dots & N_{n_c}^{n_a}\mathbf{I}_{3\times3} \end{bmatrix}, \tag{5}$$

where $\mathbf{I}_{3\times3}$ is the 3×3 identity matrix. Note that $\mathbf{N}$ is of size $3n_a \times 3n_c$.

The fine scale is simply that part of the total displacement that cannot be represented by the coarse scale. In our simulations, we will obtain the fine scale information from the displacements $\mathbf{q}_\alpha$ computed in a molecular dynamics simulation; this solution includes a part that can be represented by the coarse scale shape functions. Thus the fine scale must be defined by subtracting from $\mathbf{q}_\alpha$ the projection of the molecular dynamics solution onto the set of functions N_I. This coarse scale projection can be written as $\sum_I N_I^\alpha \mathbf{w}_I$, where $\mathbf{w}_I$ is a set of nodal degrees of freedom that minimize some measure of the difference between the coarse and total scales at an atom. We choose as this measure the sum of the squared difference at all atoms, weighted by the atomic masses m_α:

$$\sum_\alpha m_\alpha \left| \mathbf{q}_\alpha - \sum_I N_I^\alpha \mathbf{w}_I \right|^2. \tag{6}$$

It will be seen in Section 2.2 that this choice of measure allows the coarse and fine scale kinetic energies to be decoupled. This quantity can be written in matrix form by defining an atomic mass matrix $\mathbf{M}_A$ as a diagonal matrix of size $3n_a$ (for three dimensions) with the atomic masses on the diagonal

$$\mathbf{M}_A = \begin{bmatrix} m_1\mathbf{I}_{3\times3} & & & \\ & m_2\mathbf{I}_{3\times3} & & \\ & & \ddots & \\ & & & \ddots \end{bmatrix}. \tag{7}$$

The quantity in Eq. (6) can now be written

$$(\mathbf{q} - \mathbf{N}\mathbf{w})^{\mathrm{T}}\mathbf{M}_A(\mathbf{q} - \mathbf{N}\mathbf{w}). \tag{8}$$

Solving for $\mathbf{w}$ to minimize this quantity gives

$$\mathbf{w} = \mathbf{M}^{-1}\mathbf{N}^{\mathrm{T}}\mathbf{M}_A\mathbf{q}, \tag{9}$$

where the coarse scale mass matrix $\mathbf{M}$ is

$$\mathbf{M} = \mathbf{N}^{\mathrm{T}}\mathbf{M}_A\mathbf{N}. \tag{10}$$

So the fine scale $\mathbf{u}'$, which is that part of $\mathbf{q}$ that is not represented by its coarse scale projection, is

$$\mathbf{u}' = \mathbf{q} - \mathbf{N}\mathbf{w}, \tag{11}$$

$$\mathbf{u}' = \mathbf{q} - \mathbf{P}\mathbf{q}, \tag{12}$$

where the matrix $\mathbf{P}$ has been defined

$$\mathbf{P} = \mathbf{N}\mathbf{M}^{-1}\mathbf{N}^{\mathrm{T}}\mathbf{M}_A. \tag{13}$$

Note that $\mathbf{P}$ is the operator for the projection onto the coarse scale basis, and that $\mathbf{PP} = \mathbf{P}$, as required of a projection operator.

The total displacement $\mathbf{u}_\alpha$ is the sum of the coarse scale (4) and fine scale (12)

$$\mathbf{u} = \mathbf{N}\mathbf{d} + \mathbf{q} - \mathbf{P}\mathbf{q}. \tag{14}$$

The last term in the above expression we will call the "bridging scale"; it is that part of the molecular dynamics calculation that must be subtracted from the total in order to achieve a complete separation of scales.

Finally, we can define the complimentary projector $\mathbf{Q} \equiv \mathbf{I} - \mathbf{P}$:

$$\mathbf{Q} = \mathbf{I} - \mathbf{N}\mathbf{M}^{-1}\mathbf{N}^{\mathrm{T}}\mathbf{M}_A. \tag{15}$$

So that (14) can be rewritten as

$$\mathbf{u} = \mathbf{N}\mathbf{d} + \mathbf{Q}\mathbf{q}. \tag{16}$$

2.2. Multiscale Lagrangian

The set of atomic displacements, together with their time derivatives, can be used to compute the kinetic and potential energies of the total system. It is most convenient to adopt a Lagrangian mechanics description of the system, in which the Lagrangian L is the kinetic energy minus the potential energy

$$L(\mathbf{u}, \dot{\mathbf{u}}) = \frac{1}{2}\dot{\mathbf{u}}^{\mathrm{T}}\mathbf{M}_A\dot{\mathbf{u}} - U(\mathbf{u}) + \mathbf{f}_{\mathrm{ext}}^{\mathrm{T}}\mathbf{u}. \tag{17}$$

In this expression, the interatomic potential energy $U(\mathbf{u})$ is some (possibly complicated) function of the displacements only, while $\mathbf{f}_{\mathrm{ext}}$ is a vector of constant external forces acting on the atoms. Note that the potential energy U is actually a function of the positions of the atoms, obtained from adding the atoms' displacements to their initial positions; there is no assumption that the initial configuration is a regular lattice or other unstressed state. Substituting (16) into the expression for the kinetic energy gives

$$\frac{1}{2}\dot{\mathbf{u}}^{\mathrm{T}}\mathbf{M}_A\dot{\mathbf{u}} = \frac{1}{2}\dot{\mathbf{d}}^{\mathrm{T}}\mathbf{N}^{\mathrm{T}}\mathbf{M}_A\mathbf{N}\dot{\mathbf{d}} + \dot{\mathbf{d}}^{\mathrm{T}}\mathbf{N}^{\mathrm{T}}\mathbf{M}_A\mathbf{Q}\dot{\mathbf{q}} + \frac{1}{2}\dot{\mathbf{q}}^{\mathrm{T}}\mathbf{Q}^{\mathrm{T}}\mathbf{M}_A\mathbf{Q}\dot{\mathbf{q}} = \frac{1}{2}\dot{\mathbf{d}}^{\mathrm{T}}\mathbf{M}\dot{\mathbf{d}} + \frac{1}{2}\dot{\mathbf{q}}^{\mathrm{T}}\mathscr{M}\dot{\mathbf{q}}. \tag{18}$$

The last line follows through use of (10) and by noting that the middle term in the first expression is identically zero, since

$$\mathbf{N}^{\mathrm{T}}\mathbf{M}_A\mathbf{Q} = \mathbf{N}^{\mathrm{T}}\mathbf{M}_A(\mathbf{I} - \mathbf{N}\mathbf{M}^{-1}\mathbf{N}^{\mathrm{T}}\mathbf{M}_A) = \mathbf{N}^{\mathrm{T}}\mathbf{M}_A - \mathbf{M}\mathbf{M}^{-1}\mathbf{N}^{\mathrm{T}}\mathbf{M}_A = \mathbf{0}.$$

The fine scale mass matrix $\mathscr{M}$ in (18) has been defined

$$\mathscr{M} \equiv \mathbf{Q}^{\mathrm{T}}\mathbf{M}_A\mathbf{Q} = \mathbf{M}_A\mathbf{Q} = \mathbf{Q}^{\mathrm{T}}\mathbf{M}_A. \tag{19}$$

The final two equations above follows by substituting the complete expression for $\mathbf{Q}$ (15) and using the definition of the coarse scale mass matrix (10).

Thus the Lagrangian in (17) is given in terms of the finite element and MD degrees of freedom by

$$L(\mathbf{d}, \dot{\mathbf{d}}; \mathbf{q}, \dot{\mathbf{q}}) = \frac{1}{2}\dot{\mathbf{d}}^{\mathrm{T}}\mathbf{M}\dot{\mathbf{d}} + \frac{1}{2}\dot{\mathbf{q}}^{\mathrm{T}}\mathscr{M}\dot{\mathbf{q}} - U(\mathbf{N}\mathbf{d} + \mathbf{Q}\mathbf{q}) + \mathbf{f}_{\mathrm{ext}}^{\mathrm{T}}\mathbf{N}\mathbf{d} + \mathbf{f}_{\mathrm{ext}}^{\mathrm{T}}\mathbf{Q}\mathbf{q}. \tag{20}$$

An important feature of the Lagrangian in (20) is the absence of cross terms such as $\mathbf{d} \cdot \mathbf{q}$ in the kinetic energy; these terms have canceled due to the presence of the bridging scale, and the total kinetic energy is decomposed into the sum of the kinetic energy in the coarse scale plus that in the fine scale.

2.3. Multiscale equations of motion

The equations of motion can be derived from the Lagrangian according to

$$\frac{\mathrm{d}}{\mathrm{d}t}\left(\frac{\partial L}{\partial \dot{\mathbf{d}}}\right) - \frac{\partial L}{\partial \mathbf{d}} = 0, \tag{21a}$$

$$\frac{\mathrm{d}}{\mathrm{d}t}\left(\frac{\partial L}{\partial \dot{\mathbf{q}}}\right) - \frac{\partial L}{\partial \mathbf{q}} = 0. \tag{21b}$$

Substitution of (20) (temporarily ignoring the external force for simplicity) into these equations gives

$$\mathbf{M}\ddot{\mathbf{d}} = -\frac{\partial U}{\partial \mathbf{d}}, \tag{22a}$$

$$\mathscr{M}\ddot{\mathbf{q}} = -\frac{\partial U}{\partial \mathbf{q}}. \tag{22b}$$

The coupling between the scales in both equations is through the derivative of the potential energy U, which is a function of both the coarse and fine scales. These coupling terms can be put into a different form by defining a vector of the total forces on the atoms

$$\mathbf{f} = -\frac{\partial U(\mathbf{u})}{\partial \mathbf{u}}, \tag{23}$$

where $\mathbf{u}$ is the vector of total displacements, as in Eq. (16). This force $\mathbf{f}$ is the force that is computed, for instance, in a molecular dynamics simulation. Using a chain rule to expand the right-hand sides in (22a), (22b) together with (16) and (23) gives

$$\mathbf{M}\ddot{\mathbf{d}} = -\left(\frac{\partial \mathbf{u}}{\partial \mathbf{d}}\right)^{\mathrm{T}} \frac{\partial U}{\partial \mathbf{u}} = \mathbf{N}^{\mathrm{T}}\mathbf{f}, \tag{24a}$$

$$\mathscr{M}\ddot{\mathbf{q}} = -\left(\frac{\partial \mathbf{u}}{\partial \mathbf{q}}\right)^{\mathrm{T}} \frac{\partial U}{\partial \mathbf{u}} = \mathbf{Q}^{\mathrm{T}}\mathbf{f}. \tag{24b}$$

If the external forces in (20) are kept in the formulation

$$\mathbf{M}\ddot{\mathbf{d}} = \mathbf{N}^{\mathrm{T}}(\mathbf{f} + \mathbf{f}_{\mathrm{ext}}), \tag{25a}$$

$$\mathscr{M}\ddot{\mathbf{q}} = \mathbf{Q}^{\mathrm{T}}(\mathbf{f} + \mathbf{f}_{\mathrm{ext}}). \tag{25b}$$

Eq. (25b) can be rewritten using (19)

$$\mathbf{Q}^{\mathrm{T}}\mathbf{M}_A\ddot{\mathbf{q}} = \mathbf{Q}^{\mathrm{T}}(\mathbf{f} + \mathbf{f}_{\mathrm{ext}}). \tag{26}$$

Note that the matrix $\mathbf{Q}$ is singular, since multiplying a field by $\mathbf{Q}$ gives the fine scale part of the field, and many different fields can have same fine scale part; therefore the solution of and equation like $\mathbf{Q}\mathbf{u} = \mathbf{u}'$ for $\mathbf{u}$ is nonunique and $\mathbf{Q}$ must be singular. Thus, Eq. (26) does not have a unique solution, and we are free to choose any $\mathbf{q}$ that has the proper fine scale part and thus satisfies (26). However, it is clear that one such $\mathbf{q}$ is that which exactly satisfies the equation

$$\mathbf{M}_A\ddot{\mathbf{q}} = \mathbf{f} + \mathbf{f}_{\text{ext}}. \tag{27}$$

This equation is exactly the one that is solved in a molecular dynamics simulation for the atomic displacements, with the atomic forces given by (23). Therefore we can use a standard molecular dynamics simulation to obtain a solution to (27) for $\mathbf{q}$.

Note that the total scale $\mathbf{u}$ satisfies a similar equation

$$\mathbf{M}_A\ddot{\mathbf{u}} = \mathbf{f} + \mathbf{f}_{\text{ext}}. \tag{28}$$

Since $\mathbf{q}$ and $\mathbf{u}$ satisfy the same equation of motion, then if these two quantities have the same initial conditions (which they should), they are identical for all time. Thus it follows from Eq. (14) that the coarse scale is simply the projection of $\mathbf{q}$, i.e.,

$$\mathbf{N}\mathbf{d} = \mathbf{P}\mathbf{q}. \tag{29}$$

This means that the explicit solution of (25a) is completely redundant, since at any time the coarse scale can be determined by (29). This makes sense, since the MD solution for $\mathbf{q}$ should contain all of the information about the dynamics of the problem; the coarse scale is merely "along for the ride". Despite this, there are three reasons for retaining the coarse scale equation in our formulation:

(1) So far, we have been treating the problem as if the fine scale description (the MD solution) exists everywhere in the domain. As will be discussed in the next section, our goal is to limit the MD simulation to only a small part of the domain, while including the effects of the averaged fine scale in the coarse scale equation elsewhere. Retaining the coarse scale equation in the fine scale region provides a seamless transition from the MD region to the surrounding coarse scale.

(2) For some problems, such as those in which we seek a static or steady state solution, it will be beneficial to solve the coarse and fine scales iteratively. The coarse scale can describe the homogeneous part of the deformation using just a few degrees of freedom, and can be solved quickly; solution of the fine scale equation then provides a refinement to the coarse scale solution. This is similar to multigrid computational techniques in which the solution on a coarse grid is used as the initial guess for the solution on a finer grid.

(3) The coarse-fine decomposition of the solution can be used to obtain information about the simulation that is unavailable from an MD or finite element solution alone. For example, the fine scale part of the solution can be interpreted as the fluctuation about the mean (coarse scale) solution, so that the kinetic energy of the fluctuations can be related to the temperature of the system. Ensemble averages can be defined analytically by holding the coarse scales fixed and averaging over the fine scales. For example, in Appendix A we show that the ensemble averaged kinetic energy is given by

$$\langle \mathscr{K} \rangle = \frac{1}{2}\dot{\mathbf{d}}^{\mathrm{T}}\mathbf{M}\dot{\mathbf{d}} + \frac{3}{2}k_{\mathrm{B}}T(n_a - n_{\mathrm{c}}), \tag{30}$$

where n_{a} is the number of atoms, n_{c} is the number of coarse scale nodes, T is the temperature and k_{B} is Boltzmann's constant. The first term on the right-hand side is simply the coarse scale kinetic energy, while the second term can be thought of as the internal kinetic energy, i.e., the kinetic energy that is not represented by the coarse scale description. Clearly the internal kinetic energy goes to zero in the limit as the number of coarse scale nodes approaches the number of atoms, i.e., as the coarse scale mesh approaches the atomic lattice size.

Finally, it should be noted that when the coarse length scale (e.g., the finite element size) is large compared to the fine length scale (the atomic spacing), the summation in the expression for the coarse scale mass matrix (10) can be replaced with an integration. Assume that each atom can be assigned a volume ΔV_α such that the ratio $m_\alpha/\Delta V_\alpha$ is approximately constant over a distance that is large compared to the atomic spacing (i.e., more massive atoms are assigned larger volumes than smaller atoms nearby), and such that $\sum_\alpha \Delta V_\alpha$ gives the total volume of the domain. Then

$$M_{IJ} = \sum_{\alpha} m_{\alpha} N_I^{\alpha} N_J^{\alpha} = \sum_{\alpha} \frac{m_{\alpha}}{\Delta V_{\alpha}} N_I^{\alpha} N_J^{\alpha} \Delta V_{\alpha} \approx \int_V \rho(\mathbf{X}) N_I(\mathbf{X}) N_J(\mathbf{X}) \mathrm{d}\mathbf{X}. \tag{31}$$

This is the expression for the consistent mass matrix used in finite elements. Therefore, we can use a standard finite element solver to find a solution to (25a), provided that the effects of the fine scale on the right-hand side (the internal force) are properly taken into account.

3. Elimination of the fine scale degrees of freedom in the coarse scale region

In the previous sections, we have considered the scale decomposition in the case where the fine and coarse scales coexist everywhere in the domain. However, we are interested in simulations in which the fine scale is only explicitly simulated in a small region of the domain, while the coarse scale is represented on the entire domain. The effects of the fine scales that lie outside the designated MD region must be accounted for, at least in an averaged sense. Two of the most important technical issues in multiple-scale methods, boundary conditions on the MD region and the proper constitutive model in the coarse scale region, are both related to the accurate removal of these extra fine scale degrees of freedom. We will treat each of these issues separately.

3.1. Molecular dynamics boundary conditions

In the absence of external forces, Eq. (27) can be written in matrix form

$$\mathbf{M}_A \ddot{\mathbf{q}} = \mathbf{f}(\mathbf{q}), \tag{32}$$

where $\mathbf{M}_A$ is a diagonal matrix with diagonal elements given by the atomic masses (7).

Recall that, by the argument following Eq. (27), the MD degrees of freedom $\mathbf{q}$ are equivalent to the total atomic displacements $\mathbf{u}$, which can be scale-decomposed into $\bar{\mathbf{u}}$ and $\mathbf{u}'$. In order to derive boundary conditions on the MD region, we will partition the domain into two regions: region 1, where an MD simulation and coexists with the coarse scale simulation; and region 2, where only the coarse scale is solved explicitly. Designate the number of atoms in region 1 as $n_{\mathrm{a}1}$, and in region 2 as $n_{\mathrm{a}2}$. The fine scale degrees of freedom $\mathbf{u}'$ can then be partitioned into two vectors: $\mathbf{u}'_1$, the $3n_{\mathrm{a}1}$ fine scale degrees of freedom in region 1 that are to be computed explicitly; and $\mathbf{u}'_2$, the $3n_{\mathrm{a}2}$ fine scale degrees of freedom in region 2 that must be approximated. (The coefficients on the n_{a}'s are due to the three spatial dimensions.) The approximation for $\mathbf{u}'_2$ will take the form of a linearization in $\mathbf{u}'_2$, an assumption that is justified if the fine scale atomic displacements near the boundary are not too large. Linearizing the force in $\mathbf{u}'_2$ gives

$$\mathbf{f}(\mathbf{u}) \approx \mathbf{f}^*(\bar{\mathbf{u}}, \mathbf{u}'_1) - \mathbf{K}_2 \mathbf{u}'_2, \tag{33}$$

where $\mathbf{f}^*(\bar{\mathbf{u}}, \mathbf{u}'_1)$ is the nonlinear interatomic force evaluated with $\mathbf{u}'_2$ set to zero, and the stiffness matrix $\mathbf{K}_2$ is given by

$$\mathbf{K}_{2,\alpha\beta} = -\left.\frac{\partial \mathbf{f}_{\alpha}}{\partial \mathbf{u}'_{2,\beta}}\right|_{\mathbf{u}'_2 = \mathbf{0}}. \tag{34}$$

The matrix $\mathbf{K}_2$ is of a size such that subscript α ranges over all atoms, while β ranges over the atoms in region 2.

The matrices $\mathbf{M}_A$ and $\mathbf{K}_2$ and the vectors $\mathbf{q}$, $\bar{\mathbf{u}}$ and $\mathbf{f}^*$ can all be partitioned between regions 1 and 2 as was done for $\mathbf{u}'$, so that the equations of motion can be written

$$\mathbf{M}_{A1}\ddot{\mathbf{q}}_1 = \mathbf{f}_1^*(\bar{\mathbf{u}}, \mathbf{u}_1') - \mathbf{K}_{12}\mathbf{u}_2', \tag{35a}$$

$$\mathbf{M}_{A2}(\ddot{\bar{\mathbf{u}}}_2 + \ddot{\mathbf{u}}_2') = \mathbf{f}_2^*(\bar{\mathbf{u}}, \mathbf{u}_1') - \mathbf{K}_{22}\mathbf{u}_2', \tag{35b}$$

where $\mathbf{K}_{12}$ and $\mathbf{K}_{22}$ are the upper and lower partions of $\mathbf{K}_2$, respectively. Note that $\mathbf{K}_{12}$ is of size $3n_{a1} \times 3n_{a2}$, and is nonzero only where atoms in region 1 are directly coupled to atoms in region 2, i.e., near the boundary of the MD simulation.

Rearranging Eq. (35b) slightly gives

$$\ddot{\mathbf{u}}_2' + \mathbf{M}_{A2}^{-1}\mathbf{K}_{22}\mathbf{u}_2' = \mathbf{M}_{A2}^{-1}\mathbf{f}_2^*(\bar{\mathbf{u}}, \mathbf{u}_1') - \ddot{\bar{\mathbf{u}}}_2. \tag{36}$$

The degrees of freedom in $\mathbf{u}_2'$ can be eliminated by solving for them explicitly from Eq. (36), and then substituting the result back into (35a). Following the approach of Adelman and Doll [19], this is most easily done using Laplace transforms. We will use both the operator $\mathscr{L}$ and capital letters to indicate the Laplace transformation of a function in time t into a function of the variable s:

$$\mathscr{L}\{f(t)\} \equiv F(s) = \int_0^\infty \mathrm{e}^{-st} f(t)\mathrm{d}t. \tag{37}$$

Using the properties of this transformation, the equation for $\mathbf{u}_2'$ thus becomes, from (36)

$$\left[s^2\mathbf{I} + \mathbf{M}_{A2}^{-1}\mathbf{K}_{22}\right]\mathbf{U}_2'(s) = \mathbf{M}_{A2}^{-1}\mathscr{L}\left\{\mathbf{f}_2^*(\bar{\mathbf{u}}, \mathbf{u}_1')\right\} - \left(s^2\bar{\mathbf{U}}_2(s) - s\bar{\mathbf{u}}_2(0) - \dot{\bar{\mathbf{u}}}_2(0)\right) + s\mathbf{u}_2'(0) + \dot{\mathbf{u}}_2'(0). \tag{38}$$

Inverting the transform, using the fact that the product of functions in the Laplace transformed variable is equivalent to a convolution in the time variable, and resubstituting into Eq. (35a) gives an equation of motion for $\mathbf{u}_1'(t)$ that includes the effects of the unknown $\mathbf{u}_2'$ in terms of the known quantities $\bar{\mathbf{u}}$ and $\mathbf{u}_1'$:

$$\mathbf{M}_{A1}\ddot{\mathbf{q}}_1 = \mathbf{f}_1^*(\bar{\mathbf{u}}, \mathbf{u}_1') - \int_0^{\mathrm{T}} \boldsymbol{\theta}(t-\tau)\tilde{\mathbf{a}}_2(\tau)\mathrm{d}\tau + \mathbf{R}(t), \tag{39}$$

where

$$\boldsymbol{\theta}(t) = \mathscr{L}^{-1}\left\{\mathbf{K}_{12}\left[s^2\mathbf{I} + \mathbf{M}_{A2}^{-1}\mathbf{K}_{22}\right]^{-1}\right\}, \tag{40a}$$

$$\tilde{\mathbf{a}}_2(t) = \mathbf{M}_{A2}^{-1}\mathbf{f}_2^*\left(\bar{\mathbf{u}}(t), \mathbf{u}_1'(t)\right) - \ddot{\bar{\mathbf{u}}}_2(t), \tag{40b}$$

$$\mathbf{R}(t) = \dot{\boldsymbol{\theta}}(t)\mathbf{u}_2'(0) + \boldsymbol{\theta}(t)\dot{\mathbf{u}}_2'(0). \tag{40c}$$

The matrix $\boldsymbol{\theta}(t)$ is a time history kernel that captures the effects of the removed degrees of freedom. It can be derived analytically for some simple cases (e.g., see Section 5.1), or computed numerically in more complicated circumstances. The quantity $\tilde{\mathbf{a}}_2(t)$ (40b) represents the difference between the atomic accelerations in region 2 due to a force of $\mathbf{f}^*(\bar{\mathbf{u}}(t), \mathbf{u}_1'(t))$, and the actual coarse scale acceleration in that region. When the total displacement solution is fully resolved by the coarse scale alone, this difference is zero and there is no contribution from the time history integral in Eq. (39). The additional displacement vector $\mathbf{R}(t)$ is due to the initial fine scale energy in the coarse scale region. Although the exact initial conditions $\mathbf{u}_2'(0)$ and $\dot{\mathbf{u}}_2'(0)$ are unknown, they can be assumed to be known in an averaged sense and related to the temperature of the coarse scale region (see Remark 5 below).

In order to examine special cases (such as statics) and compare with other techniques, it will be convenient to rewrite Eq. (39) by integrating by parts

$$\mathbf{M}_{A1}\ddot{\mathbf{q}}_1 = \mathbf{f}_1^*(\bar{\mathbf{u}}, \mathbf{u}_1') - \boldsymbol{\beta}(0)\tilde{\mathbf{a}}_2(t) + \int_0^t \boldsymbol{\beta}(t-\tau)\frac{\partial}{\partial\tau}\tilde{\mathbf{a}}_2(\tau)\mathrm{d}\tau + \mathbf{R}_\beta(t), \tag{41}$$

where

$$\boldsymbol{\beta}(t) = \int_t^\infty \boldsymbol{\theta}(\tau)\mathrm{d}\tau, \tag{42a}$$

$$\mathbf{R}_\beta(t) = \mathbf{R}(t) + \boldsymbol{\beta}(t)\tilde{\mathbf{a}}_2(0). \tag{42b}$$

Eq. (41) gives the behavior of $\mathbf{q}_1$, the MD atomic positions, by including implicitly the effects of $\mathbf{u}_2'$ on the total forces on the atoms. Through the time history kernel convolution and the additional random force $\mathbf{R}_\beta(t)$, the removed degrees of freedom in $\mathbf{u}_2'$ are accounted for. This equation is the main result of this section, and gives the equation that is solved in the MD simulation for the degrees of freedom $\mathbf{q}$. Several remarks are in order:

(1) The first term on the right-hand side of (41), the force vector $\mathbf{f}_1^*(\bar{\mathbf{u}}, \mathbf{u}_1')$, is the nonlinear interatomic force as calculated by assuming that $\mathbf{u}_2' = 0$. In practice, this term is most easily computed by storing the positions of "ghost" atoms – atoms within one cutoff radius outside the MD region whose displacements are assumed to equal the coarse scale displacements (available from the coarse scale simulation) at all times. The force on all of the MD atoms can then be computed in the normal way.

(2) Due to the sparsity of matrix $\mathbf{K}_{12}$, the last three terms on the right-hand side of (41), which all involve $\mathbf{K}_{12}$ through the definitions in Eqs. (40a)–(40c) and (42a), (42b), are nonzero only for region 1 atoms whose forces are directly related to displacements of atoms in region 2, i.e., very close to the boundary of the MD simulation. These terms represent a force boundary condition on the MD simulation that depends in part on the coarse scale variables, coupling the two simulations.

(3) The second term on the right-hand side of Eq. (41) is a modified stiffness term due to the difference between the coarse and fine scales near the boundary. It is nonzero even for static problems.

(4) The third term on the right-hand side of Eq. (41), the time history integral, mimics the dissipation of energy from the MD simulation into the outer coarse scale region. It results in "non-reflecting" boundary conditions, allowing short wavelengths that cannot be represented by the coarse scale interpolation to pass cleanly out of the MD computational region.

(5) The last term in Eq. (41) mimics the exchange of energy between the MD and surrounding regions due to temperature differences. Note that the force $\mathbf{R}_\beta(t)$ (by Eqs. (40c) and (42b)) is in terms of the initial conditions of $\mathbf{u}_2'$, which in general are known only in an averaged sense based on the temperature of the coarse scale region. Thus, $\mathbf{R}_\beta(t)$ can be treated as a random force, the magnitude and time correlation of which depend on the temperature of the surrounding coarse scale region T. Using a technique similar to that in [20], it can be shown from Eq. (40c) that

$$\langle \mathbf{R}(t)\mathbf{R}^{\mathrm{T}}(0)\rangle = k_{\mathrm{B}}T\boldsymbol{\beta}(t)\mathbf{M}_{A2}^{-1}\mathbf{K}_{12}^{\mathrm{T}}. \tag{43}$$

Methods for applying this stochastic force, or achieving the same effects, have been developed by other authors (e.g., [21]). In the example problems in Section 5, we will assume that the temperature of the surrounding coarse scale is 0 K, so that the random forcing term can be ignored.

(6) In general, computation of the matrices $\boldsymbol{\theta}(t)$ and $\boldsymbol{\beta}(t)$ (see Eq. (40a)) involve the inversion of a matrix of a size proportional to the square of the number of degrees of freedom removed, i.e., the number of atoms in region 2. The explicit inversion of a matrix this size and its subsequent inverse Laplace transform are intractable. However, examination of Eq. (40a) shows that only a few of the entries in this inverted matrix are necessary, since as noted the matrix $\mathbf{K}_{12}$ is nonzero only for atomic pairs that span the MD boundary. For some very simple cases, the important entries of these matrices can be derived analytically.

One such case, to be treated in Section 5.1, is that of a semi-infinite 1D harmonic lattice. For more complicated cases, such as multi-dimensional solids, the important entries of $\boldsymbol{\theta}(t)$ or $\boldsymbol{\beta}(t)$ must be approximated [20] or derived numerically [22,23]. In [24], we demonstrate a simple, semi-analytical technique for the computation of $\boldsymbol{\beta}(t)$ for regular crystal lattices, and show results for the graphene and diamond structures of carbon.

Finally, we note that the initial value of $\boldsymbol{\beta}(t)$, appearing in the modified stiffness term in (41), can be rewritten using Eqs. (42a), (37), and (40a)

$$\boldsymbol{\beta}(0) = \int_0^\infty \boldsymbol{\theta}(\tau)\mathrm{d}\tau = \mathbf{K}_{12}\mathbf{K}_{22}^{-1}\mathbf{M}_{A2}. \tag{44}$$

Like $\boldsymbol{\beta}(t)$ itself, $\boldsymbol{\beta}(0)$ can only rarely be computed exactly, but can be approximated numerically for a given atomic structure.

To the authors' knowledge, the exact form derived here for Eq. (41) is new. However, it is similar to the generalized Langevin equation (GLE) boundary condition derived by Adelman and Doll [19] for the single-scale problem, with the exception of the time history integral, which for the GLE has the velocity $\dot{\mathbf{u}}_0$ in place of our $\partial\tilde{\mathbf{a}}_2/\partial\tau$. The standard form of the GLE can be recovered if we make two further assumptions: that the force $\mathbf{f}_2^*$ can be linearized in $\mathbf{u}_1'$, and that the coarse scale acceleration can be computed from just the leading order term of this linearization

$$\mathbf{f}_2^*(\bar{\mathbf{u}}, \mathbf{u}_1') \approx \mathbf{f}_2^*(\bar{\mathbf{u}}, \mathbf{0}) - \mathbf{K}_{21}\mathbf{u}_1', \tag{45a}$$

$$\ddot{\bar{\mathbf{u}}}_2 \approx \mathbf{M}_{A2}^{-1}\mathbf{f}_2^*(\bar{\mathbf{u}}, \mathbf{0}), \tag{45b}$$

where

$$\mathbf{K}_{21} = -\left.\frac{\partial \mathbf{f}_2^*}{\partial \mathbf{u}_1'}\right|_{\mathbf{u}_1'=\mathbf{0}}. \tag{46}$$

With these assumptions, the time history integral can be approximated as

$$\int_0^t \boldsymbol{\beta}(t-\tau)\frac{\partial}{\partial\tau}\tilde{\mathbf{a}}_2(\tau)\mathrm{d}\tau \approx -\int_0^t \tilde{\boldsymbol{\beta}}(t-\tau)\dot{\mathbf{u}}_1'(\tau)\mathrm{d}\tau, \tag{47}$$

where

$$\tilde{\boldsymbol{\beta}}(t) = \boldsymbol{\beta}(t)\mathbf{M}_{A2}^{-1}\mathbf{K}_{21}. \tag{48}$$

Conveniently, the matrix $\boldsymbol{\beta}(t)$ in our multiscale formulation is related in a simple way to the damping kernel in the GLE, so that analytical [20] and numerical [22,23] evaluations of the GLE kernel $\tilde{\boldsymbol{\beta}}(t)$ can be used in our multi-scale boundary condition evaluation.

In the case of statics, for which time derivatives and temperature are zero, Eq. (41) gives

$$\mathbf{0} = \mathbf{f}_1^*(\bar{\mathbf{u}}, \mathbf{u}_1') - \boldsymbol{\beta}(\mathbf{0})\tilde{\mathbf{a}}_2 = \mathbf{f}_1^*(\bar{\mathbf{u}}, \mathbf{u}_1') - \mathbf{K}_{12}\mathbf{K}_{22}^{-1}\mathbf{f}_2^*(\bar{\mathbf{u}}, \mathbf{u}_1'). \tag{49}$$

The second term on the right-hand side is an additional force term that takes into account the fact that while the fine scales $\mathbf{u}_2'$ have been eliminated from the formulation, they are not necessarily zero. If this term is neglected, care should be taken to ensure that the difference between the coarse and fine scales at the MD boundary truly is very small.

3.2. Coarse scale internal force

3.2.1. Inside the MD region

The equation for the time evolution of the coarse scale is given by (24a). In the region in which the full molecular dynamics simulation is solved, the solution of this equation is straightforward, although care should be taken to include the effects of the coarse scale when evaluating the atomic forces in the expression $\mathbf{N}^{\mathrm{T}}\mathbf{f}$. This is done by first computing the total atomic displacements according to (16), where $\mathbf{q}$ is obtained from the MD simulation, and then evaluating the forces based on these total displacements. Eq. (24a) can then be written

$$\mathbf{M}\ddot{\mathbf{d}} = \mathbf{N}^{\mathrm{T}}\mathbf{f}(\mathbf{u}) = \mathbf{N}^{\mathrm{T}}\mathbf{f}(\mathbf{N}\mathbf{d} + \mathbf{Q}\mathbf{q}). \tag{50}$$

The implementation of the computation of the internal force is simple; the same subroutine used to compute the interatomic force in the MD simulation can be used to evaluate $\mathbf{f}$ in Eq. (50).

Eq. (50) is not the only choice for the evaluation of the internal force. Because the coarse scale solution is expected to be equal to the projection of the MD solution (Eq. (29)), it might be expected that the internal force can be evaluated using the MD solution $\mathbf{q}$ for the entire total scale; this would obviate the computation of the projection $\mathbf{Q}\mathbf{q}$. In practice, however, we find that using $\mathbf{q}$ as the entire total scale in the force evaluation causes a drift between the coarse scale solution and the projection of the MD solution that is avoided when the two solutions are combined as in (50).

3.2.2. Outside the MD region

In the part of the domain in which the individual atomic displacements are not being solved using molecular dynamics, the internal force must be computed from the coarse scale solution alone, together with any information that might be known about the averaged fine scale properties (e.g., temperature). In the present work, we will assume that the coarse scale constitutive law does not depend on the temperature. Extensions to the case where the temperature is tracked in the coarse scale region using an energy equation, and the effects that temperature has on the internal force, will be pursued in future work.

The approach is similar to that used in the quasicontinuum method (see [6] for a detailed exposition). The first step is to assume that the potential energy can be written in terms of an energy density W_α, the potential energy per volume centered at atom α, so that

$$U(\mathbf{u}) = \sum_\alpha W_\alpha(\mathbf{u})\Delta V_\alpha. \tag{51}$$

The volume per atom ΔV_α is the same as that introduced in Eq. (31). Now comparing (22a) with (24a), and isolating the force at a single node I, we have

$$(\mathbf{N}^{\mathrm{T}}\mathbf{f})_I = -\frac{\partial U(\mathbf{u})}{\partial \mathbf{d}_I} = -\sum_\alpha \frac{\partial W_\alpha(\mathbf{u})}{\partial \mathbf{d}_I}\Delta V_\alpha. \tag{52}$$

The final assumption is that because the coarse scale deformation is smooth, the dependence of W_α on the coarse scale displacement $\mathbf{d}$ is only through the coarse scale deformation gradient $\bar{\mathbf{F}}$ at atom α, defined by

$$\bar{\mathbf{F}}_\alpha = \mathbf{I} + \frac{\partial \bar{\mathbf{u}}}{\partial \mathbf{X}}(\mathbf{X}_\alpha) = \mathbf{I} + \sum_I \frac{\partial N_I}{\partial \mathbf{X}}(\mathbf{X}_\alpha)\mathbf{d}_I. \tag{53}$$

Note that even though the coarse scale displacement $\bar{\mathbf{u}}$ only has a physical meaning at the atomic positions, it is a continuous function (due to the continuity of the shape functions in (2)) and we are therefore free to take its spatial derivative as in (53). Now using a chain rule on (52) gives

$$(\mathbf{N}^{\mathrm{T}}\mathbf{f})_I = -\sum_\alpha \frac{\partial W_\alpha}{\partial \bar{\mathbf{F}}_\alpha}\frac{\partial \bar{\mathbf{F}}_\alpha}{\partial \mathbf{d}_I}\Delta V_\alpha = -\sum_\alpha \frac{\partial N_I}{\partial \mathbf{X}}\bigg|_{\mathbf{X}=\mathbf{X}_\alpha}\frac{\partial W_\alpha}{\partial \bar{\mathbf{F}}_\alpha^{\mathrm{T}}}\Delta V_\alpha. \tag{54}$$

We can recognize the derivative of the energy density W with respect to $\bar{\mathbf{F}}^{\mathrm{T}}$ as the first Piola–Kirchoff stress $\mathbf{P}^K$:

$$\mathbf{P}^K(\mathbf{X}_\alpha) \equiv \frac{\partial W_\alpha}{\partial \bar{\mathbf{F}}_\alpha^{\mathrm{T}}}. \tag{55}$$

Because the functions the summation in (54) are smooth (since we have assumed that the energy density and therefore the stress are functions only of the coarse scale and the average of the fine scales), we can replace the summation by an integration, just as in Eq. (31)

$$(\mathbf{N}^{\mathrm{T}}\mathbf{f})_I \approx -\int_V \frac{\partial N_I}{\partial \mathbf{X}}(\mathbf{X})\mathbf{P}^K(\mathbf{X})\mathrm{d}\mathbf{X}. \tag{56}$$

In practice, the above integral is computed numerically by summing over a discrete set of quadrature points at the locations $\mathbf{X}_q$:

$$(\mathbf{N}^{\mathrm{T}}\mathbf{f})_I \approx -\sum_q \frac{\partial N_I}{\partial \mathbf{X}}(\mathbf{X}_q)\mathbf{P}^K(\mathbf{X}_q)w_q, \tag{57}$$

where is w_q is the quadrature weight associated with point $\mathbf{X}_q$. The stress as a function of $\bar{\mathbf{F}}$ at a point $\mathbf{X}_q$ can be computed by assuming that interatomic distances $\mathbf{r}_{\alpha\beta}$ in the deformed state are related to the initial distances $\mathbf{r}^0_{\alpha\beta}$ by the Cauchy–Born rule [6]

$$\mathbf{r}_{\alpha\beta} = \bar{\mathbf{F}}_\alpha \mathbf{r}^0_{\alpha\beta}. \tag{58}$$

With this assumption, the change in potential energy for a given $\bar{\mathbf{F}}$ can be computed, and the coarse scale internal force (57) can be evaluated.

4. Time integration with subcycling

The computational method developed in the previous sections involves a two-way exchange of information: the fine scales of the MD simulation contribute to the internal force in the coarse scale equation, and the coarse scales provide information needed to compute the additional boundary forces on the MD computation. This is very much analogous to the information exchange in a fluid–structure interaction simulation: the fluid exerts pressure and viscous forces on the solid structure, while the moving solid provides boundary conditions for the fluid flow problem. Several accurate and efficient time integration schemes have been developed for fluid–structure interaction simulations, including the option of using a time step for the fluid that is a small fraction of that used for the solid [25]. This sort of mixed time integration is ideal for our multi-scale method, in which the larger length and slower time scales associated with the coarse scale should allow us to use a much larger time step for the coarse scale simulation that for the MD. The stability of time integration methods with subcycling similar to that used here was explored in [26–28]. Although the method currently used does not allow the two simulations to be advanced in time simultaneously (since information from the end of one simulation's time step is required at the beginning of the other's), modifications may be possible that allow the exchange of information only at the beginning of each time step so that parallelism can be exploited [25].

Over each cycle, the total simulation is advanced by a time step Δt: the MD simulation is advanced by m steps of size $\Delta t/m$ (where m is a positive integer), while the coarse scale simulation is advanced through a

single step of size Δt. In our current approach, both the coarse and MD simulations are updated using an explicit central difference method. Other integration schemes should be straightforward to implement. In particular, higher order integration methods are often used in molecular dynamics codes [29]; the procedures given below can be easily adapted to use these other methods.

4.1. MD update

In our approach, the MD simulation is advanced first for m steps. This calculation requires information from the coarse scale simulation near the boundary of the MD region (see (41)), and this information is only directly available at times that are integer multiples of Δt. We will therefore use an interpolation method to approximate the coarse scale displacement and velocity at fractional time steps, by assuming that the coarse scale acceleration is constant throughout the cycle.

We will use superscripts to denote the time step, with the bracket notation $[j]$ as a shorthand for the fractional time step $n + (j/m)$, and the subcycle time step will be denoted $\Delta t_m = \Delta t/m$. The subscript Γ on coarse scale quantities indicates that those quantities are only needed close to the MD boundary. Finally, we will let $\hat{\mathbf{f}}(\mathbf{q}, \dot{\mathbf{q}}, \bar{\mathbf{u}}, \dot{\bar{\mathbf{u}}}, \mathbf{h})$ represent the entire right-hand side of Eq. (41), where $\mathbf{h}$ is used to represent time history quantities that are needed for integration. Then, assuming that $\bar{\mathbf{u}}_\Gamma^n$, $\dot{\bar{\mathbf{u}}}_\Gamma^n$, $\ddot{\bar{\mathbf{u}}}_\Gamma^n$, $\mathbf{q}^n$, $\dot{\mathbf{q}}^n$, and $\ddot{\mathbf{q}}^n$ are known, these quantities are updated in the following order:

$$\bar{\mathbf{u}}^{[j+1]} = \bar{\mathbf{u}}^{[j]} + \Delta t_m \dot{\bar{\mathbf{u}}}^{[j]} + \frac{1}{2}\Delta t_m^2 \ddot{\bar{\mathbf{u}}}^n, \tag{59a}$$

$$\dot{\bar{\mathbf{u}}}^{[j+1]} = \dot{\bar{\mathbf{u}}}^{[j]} + \Delta t_m \ddot{\bar{\mathbf{u}}}^n, \tag{59b}$$

$$\mathbf{q}^{[j+1]} = \mathbf{q}^{[j]} + \Delta t_m \dot{\mathbf{q}}^{[j]} + \frac{1}{2}\Delta t_m^2 \ddot{\mathbf{q}}^{[j]}, \tag{59c}$$

$$\dot{\tilde{\mathbf{q}}}^{[j+1]} = \dot{\mathbf{q}}^{[j]} + \Delta t_m \ddot{\mathbf{q}}^{[j]}, \tag{59d}$$

$$\ddot{\mathbf{q}}^{[j+1]} = \mathbf{M}_A^{-1}\hat{\mathbf{f}}\left(\mathbf{q}^{[j+1]}, \dot{\tilde{\mathbf{q}}}^{[j+1]}, \bar{\mathbf{u}}^{[j+1]}, \dot{\bar{\mathbf{u}}}^{[j+1]}, \mathbf{h}^{[j]}\right), \tag{59e}$$

$$\dot{\mathbf{q}}^{[j+1]} = \dot{\mathbf{q}}^{[j]} + \frac{1}{2}\Delta t_m\left(\ddot{\mathbf{q}}^{[j+1]} + \ddot{\mathbf{q}}^{[j]}\right). \tag{59f}$$

The quantity $\dot{\tilde{\mathbf{q}}}$ is a predicted atomic momentum that is used in computing the interatomic force. Note that the coarse scale updates (59a) and (59b) are chosen to give the same coarse scale displacement at step $n + 1$ as the coarse scale simulation (Eq. (60a) below). The updates in Eq. (59a)–(59f) are repeated for j from 0 to $m - 1$, after which all quantities are known at time step $n + 1$.

4.2. Coarse scale update

Once the MD quantities are obtained at time step $n + 1$, the coarse scale displacements $\mathbf{d}$, velocities $\mathbf{v}$, and accelerations $\mathbf{a}$ are advanced from time step n to $n + 1$. The internal forces are computed by combining the coarse scale displacement $\mathbf{Nd}$ with the fine scale part of the MD simulation, $\mathbf{Qq}$. In our approach, we use the MD atomic displacements at time $n + 1$ to compute the new acceleration in a central difference scheme

$$\mathbf{d}^{n+1} = \mathbf{d}^n + \Delta t \mathbf{v}^n + \frac{1}{2}\Delta t^2 \mathbf{a}^n, \tag{60a}$$

$$\mathbf{a}^{n+1} = \mathbf{M}^{-1}\mathbf{N}^{\mathrm{T}}\mathbf{f}(\mathbf{N}\mathbf{d}^{n+1} + \mathbf{Q}\mathbf{q}^{n+1}), \tag{60b}$$

$$\mathbf{v}^{n+1} = \mathbf{v}^{n} + \frac{1}{2}\Delta t(\mathbf{a}^{n} + \mathbf{a}^{n+1}). \tag{60c}$$

Finally, the coarse scale quantities at the MD boundary, $\bar{\mathbf{u}}_{\Gamma}^{n+1}$, $\dot{\bar{\mathbf{u}}}_{\Gamma}^{n+1}$, and $\ddot{\bar{\mathbf{u}}}_{\Gamma}^{n+1}$, are interpolated using the coarse scale shape functions and used in the next cycle for the MD simulation.

5. Example problems

5.1. 1D harmonic lattice

One case for which the time-history kernel of Eq. (41) can be derived analytically is that of a 1D harmonic lattice. Consider the geometry shown in Fig. 1. A chain of atoms is fixed at both ends of the chain. Each atom has mass m_{a}, with an interatomic spacing of h_{a}. We assume that the force between the atoms can be modeled with a harmonic potential, i.e., a linear spring with spring constant k. Overlaying the atomic chain is a coarse scale representation with nodal spacing h_{e}. In the figure, the 10 leftmost atoms comprise the set $\mathbf{q}_1$, with $\mathbf{q}_2$ comprising the remaining atoms, so that $n_1 = 10$ and $n_2 = n_{\mathrm{a}} - 10$.

Since the interatomic force is linear in the displacements, it can be written using a stiffness matrix: $\mathbf{f}(\mathbf{u}) = -\mathbf{K}\mathbf{u}$. The stiffness matrix $\mathbf{K}$ for this lattice is tridiagonal

$$\mathbf{K} = k\begin{bmatrix} 2 & -1 & & & & & \\ -1 & 2 & -1 & & & & \\ & -1 & 2 & -1 & & & \\ & & \ddots & \ddots & \ddots & & \\ & & & -1 & 2 & -1 & \\ & & & & -1 & 2 & \end{bmatrix}. \tag{61}$$

The matrix $\mathbf{K}_{22}$ (defined in Section 3.1) is identical in form to $\mathbf{K}$, but of size n_2^2 rather than n_{a}^2. In the limit of a very long chain of atoms (where the right side boundary is far from the boundary between $\mathbf{q}_1$ and $\mathbf{q}_2$), the important elements of the matrix $\boldsymbol{\Theta}(s) = s^2\mathbf{I} + \mathbf{M}_{A2}^{-1}\mathbf{K}_{22}$ (see Eq. (40a)) can be approximated. In particular, the first row (or column – the matrix is symmetric) of elements in $\boldsymbol{\Theta}(s)$ can be computed according to (see Appendix B)

$$\Theta_{11}(s) = \omega^{-2}Z, \tag{62a}$$

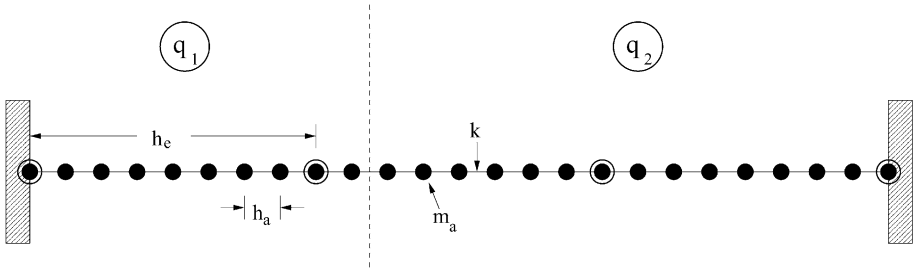

Fig. 1. 1D harmonic lattice.

$$\Theta_{1,N}(s) = Z\Theta_{1,N-1}(s), \quad N > 1, \tag{62b}$$

where

$$\omega = (k/m_a)^{1/2}, \tag{63a}$$

$$Z = \frac{1}{2}\omega^{-2}(2\omega^2 + s^2 - s(4\omega^2 + s^2)^{1/2}). \tag{63b}$$

Similarly, the inverse transforms can be computed, e.g.,

$$\theta_{n_1,1}(t) = -\frac{2m_a}{t}J_2(2\omega t), \tag{64}$$

in which J_2 is a second-order Bessel function.

Using (42a) and (48) (we will use the GLE approximation in terms of $\tilde{\boldsymbol{\beta}}$) allows a similar expression for $\tilde{\boldsymbol{\beta}}(t)$:

$$\tilde{\beta}_{n_1,n_1}(t) = \frac{k}{\omega t}J_1(2\omega t), \tag{65}$$

where J_1 is the first-order Bessel function. All other elements of $\tilde{\boldsymbol{\beta}}$ are zero, so that the boundary force is applied only at atom n_1. Plots of $\theta_{n_1,1}(t)$ and $\tilde{\beta}_{n_1,n_1}(t)$ are given in Fig. 2. Using these expressions, the equation for the degree of freedom at the MD region boundary, $\mathbf{q}_{n_1}$, can be constructed from (41) and (47); the equations for the remaining MD degrees of freedom are just the standard MD momentum equations (27). Note that because $\tilde{\boldsymbol{\beta}}(t)$ decays to zero after a few vibrational periods, the time history integral in Eq. (47) can be truncated without much loss of accuracy.

The initial condition we will use for the displacement used in the solution of this problem is a gaussian pulse of amplitude A and width σ. The pulse is truncated at $x = \pm L_c$, and shifted vertically such that the function is continuous at $x = \pm L_c$. Finally, we multiply by a fine-scale perturbation of the form

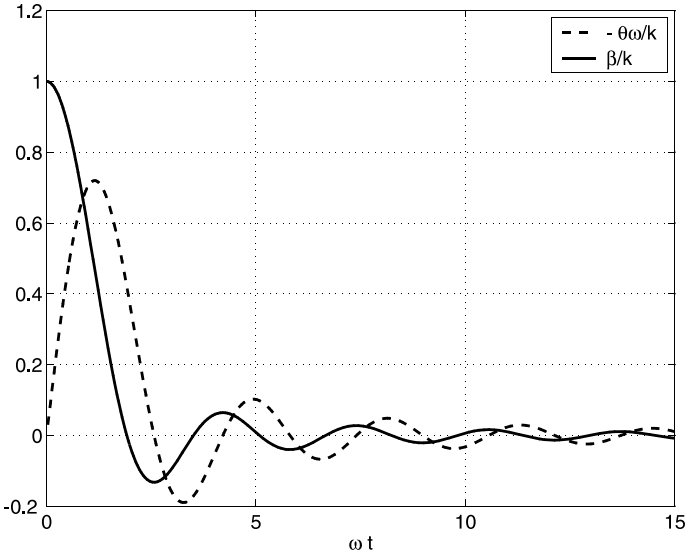

Fig. 2. $\theta_{n_1,1}(t)$ and $\tilde{\beta}_{n_1,n_1}(t)$ [Eqs. (64) and (65)] for the 1D harmonic chain.

$(1 + b\cos(2\pi x/H))$, where H is a length scale that is small compared to σ and b is the relative amplitude of the perturbation. The resulting expression for the initial displacements is

$$u(x, t = 0) = \begin{cases} A\frac{e^{-(x/\sigma)^2} - u_c}{1-u_c}\left(1 + b\cos\left(\frac{2\pi x}{H}\right)\right) & \text{if } |x| \leqslant L_c, \\ 0 & \text{if } |x| > L_c, \end{cases} \tag{66}$$

where u_c is the value of the unshifted pulse evaluated at $x = L_c$:

$$u_c = e^{-(L_c/\sigma)^2}. \tag{67}$$

The initial condition is plotted in Fig. 3, which shows both the MD and coarse scale parts of the solution; because the solution is symmetric about $x = 0$, we have only plotted the $+x$ plane. The computational domain is $-1.0 \leqslant x \leqslant 1.0$, divided into 40 linear finite elements giving $h_e = 0.05$. The region designated for MD simulation is $-0.375 \leqslant x \leqslant 0.375$; this region contains 151 atoms, so that $h = 10h_a$. The parameters chosen for the initial conditions plotted in Fig. 3 are $A = h_a = 0.005$, $b = 0.1$, $\sigma = 10h_a$, $L_c = 5\sigma$, and $H = \sigma/4$. Note that the vertical axis in Fig. 3 represents the displacement in the x direction, since the problem is in 1D.

The simulation is run with a coarse scale time step of $\Delta t = 0.1h_e/c$, where $c = h_a\sqrt{k/m_a}$ is the wave speed in the lattice. The MD simulation undergoes 10 subcycles for every step taken by the coarse scale. In order to demonstrate the effects of the MD boundary condition, the wave is propagated using two different boundary conditions at the MD region boundary. In the first (Fig. 4), the boundary condition is applied by simply setting the MD velocity at the boundary equal to the coarse scale velocity evaluated at the boundary atoms. This leads to an internal reflection of the fine scale perturbation, since the fine scale waves cannot be represented on the coarse scale grid. The correct method of applying boundary conditions is to use Eq. (41) to evaluate the force at the MD boundary; these results are shown in Fig. 5. When the boundary condition is correctly applied, the fine scale waves pass out of the MD region properly at the same time as the coarse scale pulse propagates into the coarse scale region.

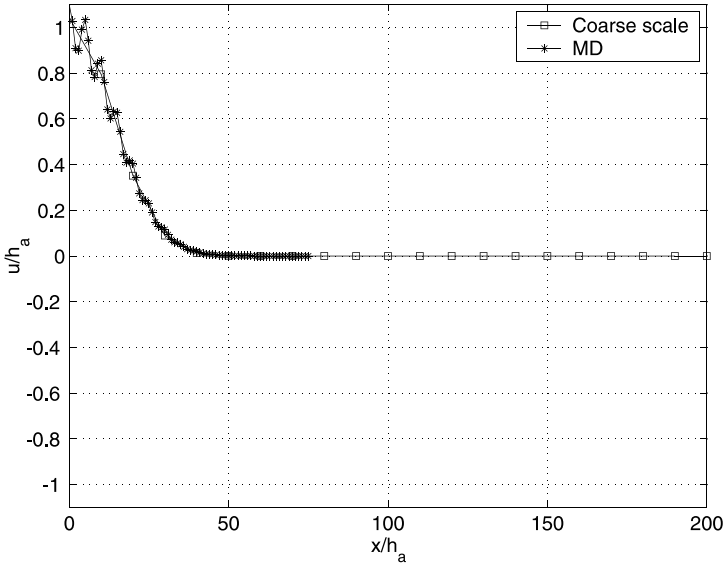

Fig. 3. Initial conditions [Eq. (66)] for 1D example problem.

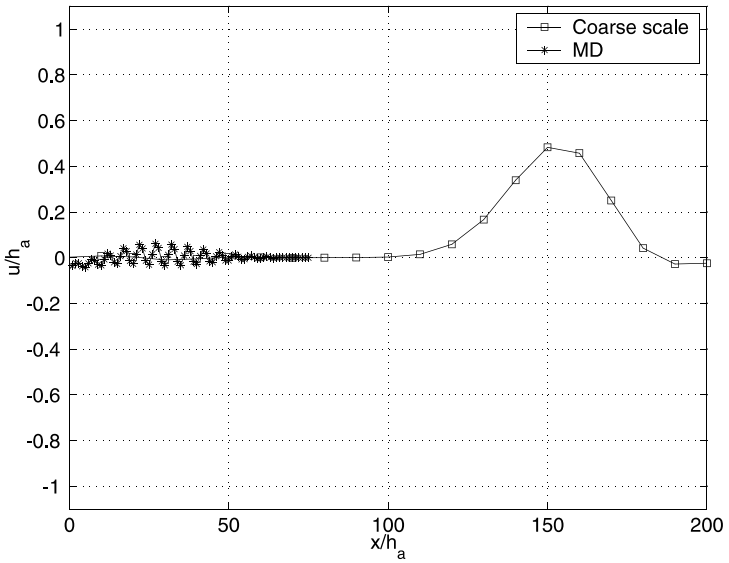

Fig. 4. 1D example problem at $t = 15.0h/c$ when the coarse scale velocity solution is applied directly as the MD boundary condition.

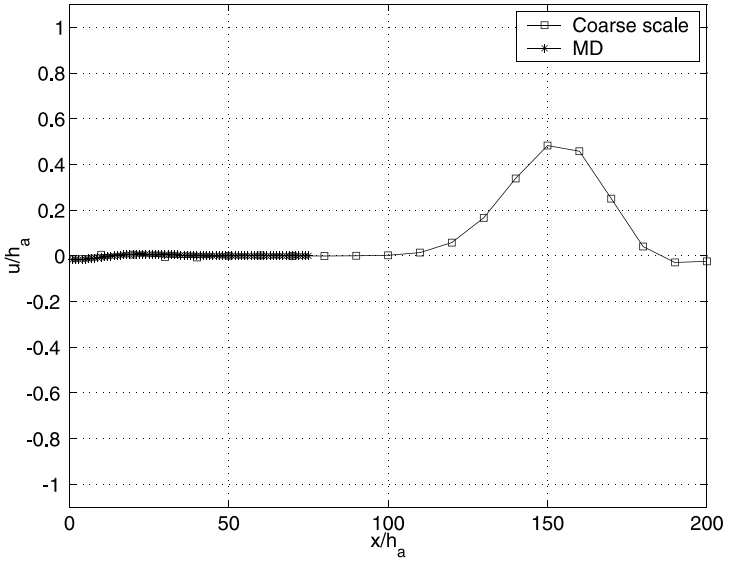

Fig. 5. 1D example problem at $t = 15.0h/c$ when Eq. (41) is used to compute boundary forces on the MD region.

One way to characterize the results of this example problem is by examining the time dependence of the total energy in the MD region. This energy is defined as the kinetic energy of all of the atoms in the MD region, plus the potential energy of all of the bonds between these atoms (including half of the potential energy in each of the bonds that spans the outer boundary of the MD region). Ideally, all of the energy that is in this region initially passes out into the surrounding coarse scale region. Fig. 6 shows the transfer of energy for the two solutions above (Figs. 4 and 5) along with the exact energy transfer out of this region as

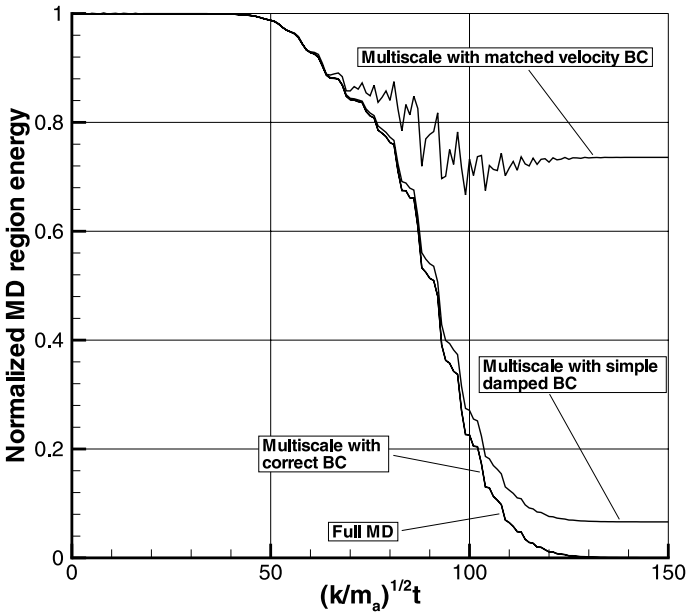

Fig. 6. Total energy of the MD region, normalized by the initial energy, as a function of time. Results shown are for the problem of the 1D harmonic oscillator. Note that the curve for the multiscale solution (41) with the correct BC is indistinguishable from the full MD solution. The simple damped BC uses the damping coefficient defined in Eq. (69).

computed from a full MD simulation of the entire domain. Also shown in this figure is the energy transfer resulting from an approximation of the time history integral in Eq. (41) as a damping term that is proportional to the velocity at time t; i.e., if we approximate $\tilde{\boldsymbol{\beta}}(t)$ as

$$\tilde{\boldsymbol{\beta}}(t) \approx 2\bar{\boldsymbol{\beta}}\delta(t-\tau), \tag{68}$$

where

$$\bar{\boldsymbol{\beta}} = \int_0^\infty \tilde{\boldsymbol{\beta}}(t)\mathrm{d}t, \tag{69}$$

then we can replace the time history integral in (47) with $-\bar{\boldsymbol{\beta}}\dot{\mathbf{u}}'_1(t)$.

Fig. 6 shows that while the velocity-matching boundary condition causes energy to be artificially retained in the MD region, the proper boundary condition treatment gives an energy transfer to the outer region that is indistinguishable from that of the full MD solution, with all of the energy eventually leaving the MD region. The linear damping boundary condition approximation allows more than 90% of the energy to leave the MD region, but still results in a small amount of internal reflection and retention of energy.

5.2. 1D anharmonic lattice

Because Eq. (41) is derived by linearizing in the fine scale deformation, it is worthwhile to examine the performance of the method when the interatomic potential is anharmonic, i.e., when the force between atoms is a nonlinear function of the distance between atoms. As a simple example, we modify the springs between atoms in the previous example so that the force-displacement relationship is nonlinear. The spring force between any two atoms α and $\alpha+1$ is given by

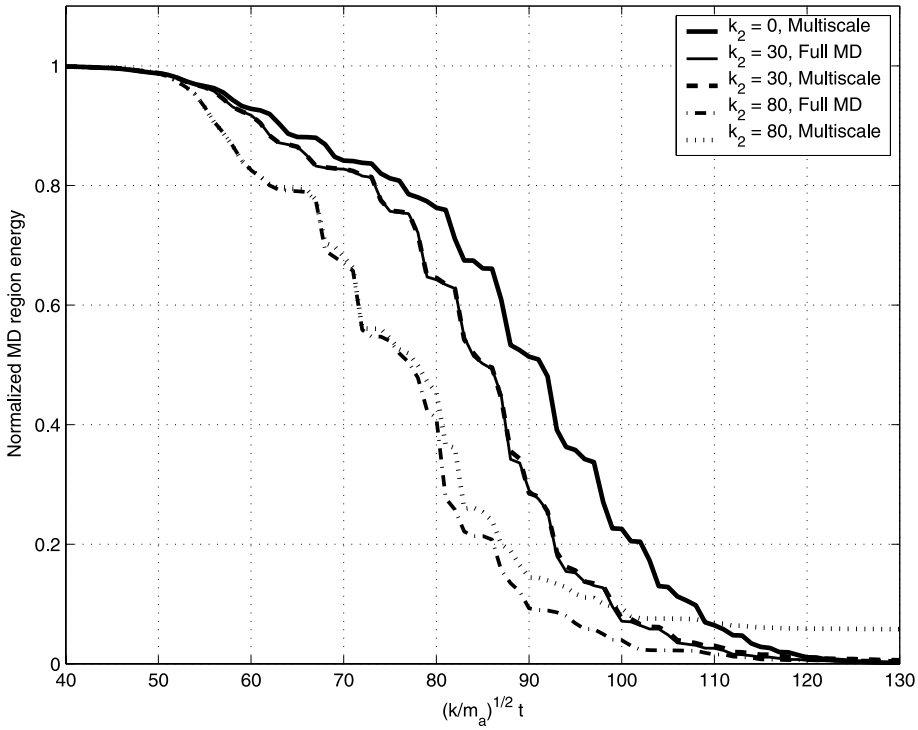

Fig. 7. Total energy of the MD region, normalized by the initial energy, as a function of time. Results are shown for several values of k_2 for the nonlinear harmonic oscillator. Note that the multiscale and full MD solutions are indistinguishable for $k_2 = 0$, and very close for $k_2 = 30$.

$$f_{\alpha,\alpha+1} = k(u_{\alpha+1} - u_\alpha) + k_2(u_{\alpha+1} - u_\alpha)^3 \tag{70}$$

so that choosing $k_2 = 0$ gives a harmonic lattice as in the previous example. The simulation then proceeds in exactly the same way as for the harmonic case, with (70) used to compute the interatomic forces for the MD atoms and the stress (equivalent to the force in the 1D case) at quadrature points in the coarse scale simulation. In the evaluation of the boundary condition for the MD simulation (41), we use the same function $\tilde{\boldsymbol{\beta}}(t)$ as was used for the linear case [Eq. (65)], without modification to take into account the dependence of the stiffness on displacement due to the nonlinearity.

The simulation was run for several values of k_2 using the same initial conditions as for the linear case. The development of the energy in the MD region for $k_2 = 30k/h_a^2$ and $k_2 = 80k/h_a^2$ is shown in Fig. 7, compared with both the $k_2 = 0$ case and with the "correct" results from a full MD simulation. The energy transfer is very good compared with the full MD solution for the $k_2 = 30k/h_a^2$ case, even though the effect of the nonlinearity is large enough to give a solution that differs noticeably from the linear case. The solution for $k_2 = 80k/h_a^2$ displays some internal reflection of small scale waves from the boundary; however, the difference from the correct solution is probably small enough to be tolerated in most problems.

6. Conclusions and future research

We have put forward a method for coupling molecular dynamics and continuum mechanics computations in a single multiple-scale simulation. In this approach, the total atomic displacement is taken to be the

sum of the two separate solutions minus the projection of the MD solution onto the coarse scale basis functions (the so-called "bridging scale"). This formulation leads to a natural decoupling of the kinetic energies of the two solutions. The coupling between the simulations is twofold: through the dependence of the coarse scale internal force on the fine scale degrees of freedom, and through the effects of the fine scale degrees of freedom that have been eliminated from the problem on the atoms at the boundary of the MD region. Using our technique, simulations can be performed using a different time step for each solution, so that the coarse scale time step need not be limited to the time scale characterizing atomic vibrations in the MD simulation.

The ability to apply this method as accurately as possible depends in part on the availability of an expression for the function $\boldsymbol{\beta}(t)$ in Eq. (41), which in effect provides boundary conditions on the MD simulation. In our example problems in Section 5, we have utilized an exact solution for the 1D semi-infinite harmonic lattice. In multiple dimensions, exact solutions can be derived in a similar way for periodic crystal structures [24], as long as the MD region boundary is perfectly planar and there are no deviations from the assumption that the material is periodic and semi-infinite, such as dislocations or a nearby free surface. For more complicated situations, where analytical solutions for $\boldsymbol{\beta}(t)$ are impossible, $\boldsymbol{\beta}(t)$ must be approximated either through analytical techniques or numerically. For example, Adelman and Doll [20] derived the Laplace transform of the time integration kernel for a Debye solid, and although a closed form in the time domain is not available, it can be approximated using numerical methods. Cai et al. [22] show how the damping kernel in a generalized Langevin equation can be computed from a molecular dynamics simulation of an extended region. Of course, in multiple dimensions the time history integral may be difficult to compute, even with an expression for $\boldsymbol{\beta}(t)$ in hand, since it requires storage of values of $\dot{\mathbf{q}}(t)$ and $\ddot{\bar{\mathbf{u}}}(t)$ over a number of time steps. It is desireable, therefore, to reduce the number of values that must be stored to a minimum by making an approximation to the time history integral that involves fewer terms. This is the approach taken by E and Huang [23], who minimize boundary reflection in an MD simulation by replacing the time history integral with a reduced sum of history terms, with weights chosen to give optimum behavior.

A very interesting direction for future research is the development of an energy equation that can describe the time dependence of the internal energy given in Eq. (30). At the fine scale, there is no need for a separate concept of temperature or internal energy, since all of the dynamics are contained in the momentum equation for the atoms (27). However, in many problems of interest (such as fracture, or surface friction), a large amount of fine scale energy is generated in the region to be simulated with MD, and the propagation of this energy as heat into the coarse scale region is of great importance in accurately simulating the dynamics. In the fine scale region, the flow of energy between coarse and fine scales due to nonlinear interactions is automatically handled by the coupling (another advantage to tracking the coarse scale even in the MD region). At the boundaries of the fine scale region, however, the internal energy that passes out of the MD simulation (due to the boundary conditions in Eq. (41)) should be tracked in the coarse scale region through the solution of an energy equation. In turn, the temperature of the coarse scale affects the fine scale dynamics through the random forces in (41). Currently, it seems unlikely that a tractable equation for the internal energy of the coarse scale can be derived directly from the interatomic potential, as can be done for the coarse scale constitutive law, without resorting to substantial approximation; the problem parallels that of development of Reynolds averaged equations for the subgrid stress in turbulence simulations. However, it should be possible to solve some form of a heat conduction equation in the coarse scale, with material properties chosen to match those of the atomic lattice as closely as possible, in order to track the temperature in the coarse scale region.

Finally, it should be noted that while we have concentrated on problems in solid mechanics, in which it is easy to treat the continuum material with a Lagrangian formulation and thus treat a closed set of atoms in the MD simulation, it should be possible to extend the method to multiple-scale problems in fluid dynamics, in which the continuum is treated with an Eulerian description. For this case, it will be necessary to add and remove atoms at the boundaries of the MD simulation in a way that is consistent with the averaged

properties of the fluid given by the coarse scale being solved concurrently. Some care must be taken in this to ensure that an atom that is inserted into the simulation does not increase the potential energy by too large an amount through its proximity to other atoms, while still satisfying the known coarse scale values of velocity, density and temperature. Some form of Monte Carlo scheme may be called for, in which trial insertions of atoms are rejected if they lead to too large a difference in local properties from the coarse scale values.

Although the example problems shown in this paper have been limited to 1 dimension, the method presented here has already been successfully applied to the simulation of buckling of a carbon nanotube under axial compression [30,31]. We believe that the method shows promise for use in many problems in which neither MD nor continuum descriptions alone are sufficient for simulating a complicated problem, including nanoindentation, solid fracture, and friction, all of which involve the interaction of multiple length and time scales.

Acknowledgements

We would like to thank Dong Qian, Ted Belytschko, Harold Park, Eduard Karpov and Hiroshi Kadowaki for many helpful discussions. The support of the National Science Foundation is also gratefully acknowledged.

Appendix A. Ensemble-averaged kinetic energy

In a physical experiment, it is generally not possible to observe the fine scale details of atomic motion. Of course, it is the atomic interaction at the nanoscale that is at the root of all macroscopic motion, even though it is only some average of the atomic-scale motion that can in most cases be observed. In our multiple-scale decomposition, we equate the coarse scales with the observable quantities, while the fine scale contribution is taken into account in an averaged sense.

Formally, this averaging is done through an ensemble average. We will assume that our systems can be described by the canonical ensemble. The total energy of the system is

$$E(\mathbf{d},\dot{\mathbf{d}};\mathbf{q},\dot{\mathbf{q}}) = \frac{1}{2}\dot{\mathbf{d}}^{\mathrm{T}}\mathbf{M}\dot{\mathbf{d}} + \frac{1}{2}\dot{\mathbf{q}}^{\mathrm{T}}\mathscr{M}\dot{\mathbf{q}} + U(\mathbf{u}). \tag{A.1}$$

In the canonical ensemble, probability distribution functions have the form

$$\rho(\mathbf{u},\dot{\mathbf{u}}) \propto \mathrm{e}^{-\beta E}, \tag{A.2}$$

where $\beta = (k_{\mathrm{B}}T)^{-1}$, k_{B} being Boltzmann's constant and T the temperature of the system. Since the averages of interest are only over the fine scale variables, we will assume that the coarse scale variables can be held fixed when performing the averaging operation. Thus the ensemble average of the kinetic energy $\mathscr{K}$ is can be computed according to

$$\begin{aligned}\langle \mathscr{K}(\dot{\mathbf{d}},\dot{\mathbf{q}})\rangle &= \frac{\int_{-\infty}^{\infty}\int_{-\infty}^{\infty}\mathscr{K}(\dot{\mathbf{d}},\dot{\mathbf{q}})\exp\left[-\beta\left(\frac{1}{2}\dot{\mathbf{d}}^{\mathrm{T}}\mathbf{M}\dot{\mathbf{d}}+\frac{1}{2}\dot{\mathbf{q}}^{\mathrm{T}}\mathscr{M}\dot{\mathbf{q}}+U(\mathbf{u}(\mathbf{d},\mathbf{q}))\right)\right]\mathrm{d}\mathbf{q}\mathrm{d}\dot{\mathbf{q}}}{\int_{-\infty}^{\infty}\int_{-\infty}^{\infty}\exp\left[-\beta\left(\frac{1}{2}\dot{\mathbf{d}}^{\mathrm{T}}\mathbf{M}\dot{\mathbf{d}}+\frac{1}{2}\dot{\mathbf{q}}^{\mathrm{T}}\mathscr{M}\dot{\mathbf{q}}+U(\mathbf{u}(\mathbf{d},\mathbf{q}))\right)\right]\mathrm{d}\mathbf{q}\mathrm{d}\dot{\mathbf{q}}} \\ &= \frac{\int_{-\infty}^{\infty}\left(\frac{1}{2}\dot{\mathbf{d}}^{\mathrm{T}}\mathbf{M}\dot{\mathbf{d}}+\frac{1}{2}\dot{\mathbf{q}}^{\mathrm{T}}\mathscr{M}\dot{\mathbf{q}}\right)\exp\left[-\frac{1}{2}\beta\dot{\mathbf{q}}^{\mathrm{T}}\mathscr{M}\dot{\mathbf{q}}\right]\mathrm{d}\dot{\mathbf{q}}}{\int_{-\infty}^{\infty}\exp\left[-\frac{1}{2}\beta\dot{\mathbf{q}}^{\mathrm{T}}\mathscr{M}\dot{\mathbf{q}}\right]\mathrm{d}\dot{\mathbf{q}}}.\end{aligned} \tag{A.3}$$

The evaluation of this integral is standard in statistical mechanics [32]; the result is

$$\langle \mathscr{K}(\dot{\mathbf{d}}, \dot{\mathbf{q}}) \rangle = \frac{1}{2}\dot{\mathbf{d}}^{\mathrm{T}}\mathbf{M}\dot{\mathbf{d}} + \frac{1}{2\beta}\mathrm{Tr}(\mathscr{M}), \tag{A.4}$$

$$\langle \mathscr{K}(\dot{\mathbf{d}}, \dot{\mathbf{q}}) \rangle = \frac{1}{2}\dot{\mathbf{d}}^{\mathrm{T}}\mathbf{M}\dot{\mathbf{d}} + \frac{3}{2}k_{\mathrm{B}}T(n_{\mathrm{a}} - n_{\mathrm{c}}), \tag{A.5}$$

where n_{a} is the number of atoms and n_{c} is the number of coarse scale nodes.

Appendix B. Inverting the matrix $\boldsymbol{\Theta}(s) = (s^2\mathbf{I} + \mathrm{M}_{A2}\mathrm{K}_{22})$ for the 1D harmonic oscillator

The matrix to be inverted is tridiagonal, with main diagonal elements $2\omega^2 + s^2$ and off-diagonal elements $-\omega^2$ (where $\omega = \sqrt{k/m_{\mathrm{a}}}$). We will begin by inverting a matrix of size N, and then examine the limit as $N \to \infty$.

Let us take $N = 4$. We can find the first column of the inverse matrix $\boldsymbol{\Theta}(s)$ by solving a matrix problem

$$\begin{bmatrix} a & b & 0 & 0 \\ b & a & b & 0 \\ 0 & b & a & b \\ 0 & 0 & b & a \end{bmatrix} \begin{bmatrix} \Theta_{11} \\ \Theta_{21} \\ \Theta_{31} \\ \Theta_{41} \end{bmatrix} = \begin{bmatrix} 1 \\ 0 \\ 0 \\ 0 \end{bmatrix}, \tag{B.1}$$

where $a = 2\omega^2 + s^2$ and $b = -\omega^2$. The solution to this equation is

$$\Theta_{11} = \left(a - b^2 \left(a - b^2 \left(a - \frac{b^2}{a} \right)^{-1} \right)^{-1} \right)^{-1}, \tag{B.2a}$$

$$\Theta_{21} = -b \left(a - b^2 \left(a - \frac{b^2}{a} \right)^{-1} \right)^{-1} \Theta_{11}, \tag{B.2b}$$

$$\Theta_{31} = -b \left(a - \frac{b^2}{a} \right)^{-1} \Theta_{21}, \tag{B.2c}$$

$$\Theta_{41} = -\frac{b}{a}\Theta_{31}. \tag{B.2d}$$

By the emerging pattern it is clear that as $N \to \infty$, the solution takes the form

$$\Theta_{11} = -\frac{Z}{b}, \tag{B.3a}$$

$$\Theta_{1,N} = Z\boldsymbol{\Theta}_{1,N-1}, \quad N > 1, \tag{B.3b}$$

where Z represents a continued fraction

$$Z = -\cfrac{b}{a - \cfrac{b^2}{a - \cfrac{b^2}{a - \cdots}}} \tag{B.4}$$

or

$$Z = -\frac{b}{a + bZ}. \tag{B.5}$$

Solving for Z gives

$$Z = -\frac{1}{2b}\left(a - \sqrt{a^2 - 4b^2}\right). \tag{B.6}$$

Substituting the values for a and b into this expression and (B.3a) results in Eqs. (62a) and (63a).

References

[1] P. Gumbsch, R.M. Cannon, Atomistic aspects at brittle fracture, MRS Bull. 25 (5) (2000) 15–20.
[2] M.H. Muser, Towards an atomistic understanding of solid friction by computer simulations, Comput. Phys. Commun. 146 (1) (2002) 54–62.
[3] M.F. Horstemeyer, M.I. Baskes, S.J. Plimpton, Computational nanoscale plasticity simulations using embedded atom potentials, Theor. Appl. Fract. Mech. 37 (1-3) (2001) 49–98.
[4] F.F. Abraham, J.Q. Broughton, N. Bernstein, E. Kaxiras, Spanning the continuum to quantum length scales in a dynamic simulation of brittle fracture, Europhys. Lett. 44 (6) (1998) 783–787.
[5] J.Q. Broughton, F.F. Abraham, N. Bernstein, E. Kaxiras, Concurrent coupling of length scales: methodology and application, Phys. Rev. B 60 (4) (1999) 2391–2403.
[6] E.B. Tadmor, M. Ortiz, R. Phillips, Quasicontinuum analysis of defects in solids, Philos. Mag. A 73 (6) (1996) 1529–1563.
[7] E.B. Tadmor, R. Phillips, M. Ortiz, Mixed atomistic and continuum models of deformation in solids, Langmuir 12 (19) (1996) 4529–4534.
[8] V.B. Shenoy, R. Miller, E.B. Tadmor, R. Phillips, M. Ortiz, Quasicontinuum models of interfacial structure and deformation, Phys. Rev. Lett. 80 (4) (1998) 742–745.
[9] R. Miller, M. Ortiz, R. Phillips, V. Shenoy, E.B. Tadmor, Quasicontinuum models of fracture and plasticity, Eng. Fract. Mech. 61 (3–4) (1998) 427–444.
[10] R. Miller, E.B. Tadmor, R. Phillips, M. Ortiz, Quasicontinuum simulation of fracture at the atomic scale, Model Simulat. Mater. Sci. 6 (5) (1998) 607–638.
[11] M. Ortiz, A.M. Cuitino, J. Knap, M. Koslowski, Mixed atomistic continuum models of material behavior: the art of transcending atomistics and informing continua, MRS Bull. 26 (3) (2001) 216–221.
[12] V. Shenoy, R. Phillips, Finite temperature quasicontinuum methods, in: V. Bulatov, T.d.l. Rubia, R. Phillips, E. Kaxiras, N. Ghoniem (Eds.), Multiscale Modelling of Materials, Materials Research Society, Warrendale, PA, 1999, pp. 465–471.
[13] S. Li, W.K. Liu, Meshfree and particle methods and their applications, Appl. Mech. Rev. 55 (1) (2002) 1–34.
[14] T.J.R. Hughes, G.R. Feijoo, L. Mazzei, J.B. Quincy, The variational multiscale method – a paradigm for computational mechanics, Comput. Meth. Appl. Mech. Eng. 166 (1–2) (1998) 3–24.
[15] K. Garikipati, T.J.R. Hughes, A variational multiscale approach to strain localization – formulation for multidimensional problems, Comput. Meth. Appl. Mech. Eng. 188 (1–3) (2000) 39–60.
[16] W.K. Liu, R.A. Uras, Y. Chen, Enrichment of the finite element method with the reproducing kernel particle method, J. Appl. Mech-T ASME 64 (4) (1997) 861–870.
[17] G.J. Wagner, W.K. Liu, Hierarchical enrichment for bridging scales and mesh-free boundary conditions, Int. J. Numer. Meth. Eng. 50 (3) (2001) 507–524.
[18] W.M. Han, G.J. Wagner, W.K. Liu, Convergence analysis of a hierarchical enrichment of dirichlet boundary conditions in a mesh-free method, Int. J. Numer. Meth. Eng. 53 (6) (2002) 1323–1336.
[19] S.A. Adelman, J.D. Doll, Generalized langevin equation approach for atom/solid-surface scattering – collinear atom/harmonic chain model, J. Chem. Phys. 61 (10) (1974) 4242–4245.
[20] S.A. Adelman, J.D. Doll, Generalized langevin equation approach for atom-solid-surface scattering – general formulation for classical scattering off harmonic solids, J. Chem. Phys. 64 (6) (1976) 2375–2388.
[21] H.J.C. Berendsen, J.P.M. Postma, W.F. Vangunsteren, A. Dinola, J.R. Haak, Molecular-dynamics with coupling to an external bath, J. Chem. Phys. 81 (8) (1984) 3684–3690.
[22] W. Cai, M. de Koning, V.V. Bulatov, S. Yip, Minimizing boundary reflections in coupled-domain simulations, Phys. Rev. Lett. 85 (15) (2000) 3213–3216.

[23] W. E, Z.Y. Huang, Matching conditions in atomistic-continuum modeling of materials, Phys. Rev. Lett. 87 (13) (2001), art. no. 135501.
[24] G.J. Wagner, E. Karpov, W.K. Liu, Molecular dynamics boundary conditions for regular crystal lattices, Comput. Meth. Appl. Mech. Eng., in press.
[25] C. Farhat, M. Lesoinne, Two efficient staggered algorithms for the serial and parallel solution of three-dimensional nonlinear transient aeroelastic problems, Comput. Meth. Appl. Mech. Eng. 182 (3–4) (2000) 499–515.
[26] T. Belytschko, H. Yen, R. Mullen, Mixed methods for time integration, Comput. Meth. Appl. Mech. Eng. 17-8 (1979) 259–275.
[27] W.K. Liu, T. Belytschko, Mixed-time implicit–explicit finite-elements for transient analysis, Comput. Struct. 15 (4) (1982) 445–450.
[28] W.K. Liu, Development of mixed time partition procedures for thermal-analysis of structures, Int. J. Numer. Meth. Eng. 19 (1) (1983) 125–140.
[29] J.M. Haile, Molecular Dynamics Simulation: Elementary Methods, Wiley, New York, 1992.
[30] D. Qian, Multiscale simulation of the mechanics of carbon nanotubes, Ph.D. Thesis, Northwestern University, 2002.
[31] D. Qian, G.J. Wagner, W.K. Liu, A multicale projection method for the analysis of carbon nanotubes, in press.
[32] F. Reif, Fundamentals of Statistical and Thermal Physics, McGraw-Hill, New York, 1965.